MedChemComm

Macrocyclic derivatives of 6-methyluracil as ligands of the peripheral anionic site of acetylcholinesterase

Journal:	*Medicinal Chemistry Communications*
Manuscript ID:	MD-CAR-05-2014-000225.R2
Article Type:	Concise Article
Date Submitted by the Author:	18-Aug-2014
Complete List of Authors:	Semenov, Vyacheslav; A.E.Arbuzov Institute of Organic and Physical Chemistry, Kazan Scientific Center, Russian Academy of Sciences, Nucleotide bases chemistry Giniyatullin, Rashit; A.E.Arbuzov Institute of Organic and Physical Chemistry, Kazan Scientific Center, Russian Academy of Sciences, Lushchekina, Sofya; N.M. Emanuel Institute of Biochemical Physics, Kots, Ekaterina; Moscow State University, Petrov, Konstantin; A.E.Arbuzov Institute of Organic and Physical Chemistry, Kazan Scientific Center, ; Kazan Institute of Biochemistry and Biophysics, ; Kazan Federal University, Nikitashina, Alexandra; A.E.Arbuzov Institute of Organic and Physical Chemistry, Kazan Scientific Center, Russian Academy of Sciences, ; Kazan Institute of Biochemistry and Biophysics, ; Kazan Federal University, Minnekhanova, Oksana; A.E.Arbuzov Institute of Organic and Physical Chemistry, Kazan Scientific Center, Russian Academy of Sciences, Zobov, Vladimir; A.E.Arbuzov Institute of Organic and Physical Chemistry, Kazan Scientific Center, Russian Academy of Sciences, ; Kazan Federal University, Nikolsky, Evgeny; A.E.Arbuzov Institute of Organic and Physical Chemistry, Kazan Scientific Center, Russian Academy of Sciences, ; Kazan Institute of Biochemistry and Biophysics, ; Kazan Federal University, ; Kazan State Medical University, Masson, Patrick; Kazan Federal University, ; DYNAMOP, Institut de Biologie Structurale, Reznik, Vladimir; A.E.Arbuzov Institute of Organic and Physical Chemistry, Kazan Scientific Center, Russian Academy of Sciences,

Journal Name

RSCPublishing

ARTICLE

Macrocyclic Derivatives of 6-Methyluracil as Ligands of the Peripheral Anionic Site of Acetylcholinesterase

Cite this: DOI: 10.1039/x0xx00000x

Received 00th January 2012,
Accepted 00th January 2012

DOI: 10.1039/x0xx00000x

www.rsc.org/

Vyacheslav E. Semenov,*[a] Rashit Kh. Giniyatullin,[a] Sofya V. Lushchekina,[b] Ekaterina D. Kots,[c] Konstantin A. Petrov,[a,d,e] Alexandra D. Nikitashina,[a,d,e] Oksana A. Minnekhanova,[a] Vladimir V. Zobov,[a,e] Evgeny E. Nikolsky,[a,d,e,f] Patrick Masson[e,g] and Vladimir S. Reznik[a]

Novel pyrimidinophanes possessing two o-nitrobenzylethyldialkylammonium heads bridging with different spacers were prepared. Pyrimidinophanes **2a**, **2b** and **3** are reversible inhibitors of cholinesterases. They show a very good selectivity for human acetylcholinesterase (AChE), with inhibitory power 100-200 times higher than for human butyrylcholinesterase (BChE). Docking simulations indicate specific binding of pyrimidinophanes **2a** and **4** on the peripheral anionic site of AChE. Other compounds bind to the active center of AChE as well as to the peripheral anionic site. These compounds are dual binding site inhibitors. Pyrimidinophane **2b** and its acyclic counterpart **1** were tested in animal model of myasthenia gravis and may be considered as valuable candidates for the treatment of pathological muscle weakness syndromes.

Introduction

Acetylcholinesterase (AChE) inhibitors are widely used in medicine for pharmacological correction of cholinergic neurotransmission pathologies.[1,2] The efficacy of anti-AChE drugs is based on their ability to potentiate the effects of acetylcholine (ACh) due to a decrease in the rate of AChE-catalyzed hydrolysis of ACh. Under these conditions, extension of the lifetime of ACh molecules is able to compensate decreases in the density of functionally active cholinergic receptors in diseases such as myasthenia gravis (MG) and Alzheimer's disease.

Crystallographic studies showed that the active site of AChE is located at the bottom of a deep gorge.[3] It was shown that, in addition to its catalytic center, AChE has other sites that are crucial for the proper functioning of the enzyme. In particular, the so-called peripheral anionic site (PAS) located at the entrance of the active site gorge is responsible for: (1) allosteric modulation of the catalytic center; (2) enzyme inhibition at high substrate concentration; 3) and non-catalytic functions such as enhancement of cell adhesion and neurite outgrowth.[4] Especially interesting is the relationship between the PAS and pathological beta-amyloid deposition. This led to a new hypothesis for rational design of more effective anti-Alzheimer drugs.[5]

Unfortunately, the functions of the PAS of AChE have never been investigated in living organisms. At the moment all data were obtained only *in vitro* or in cell cultures because the assortment of AChE PAS ligands that can be used *in vivo* is extremely limited. Customary used PAS ligands are: (i) propidium and thioflavine (initially developed as fluorescent probes for nucleic acids and apoptosis process); (ii) gallamine, d-tubocurarine (myorelaxants) and BW284C51 (that also blocks muscle nicotinic receptors)[6]); (iii) fasciculin-2 (a 61 amino acid peptide from the venom of the green mamba).[7] Low selectivity of these compounds for AChE in vivo (exept fasciculin) makes their application as therapeutic agents unpromising. Fasciculin inhibits AChE in the nanomolar range. However, multiple administrations of this toxin may induce immune response in animal models.

Several "dual binding site" inhibitors of AChE have also been described. These inhibitors bind to both active site (usually with higher affinity).[8] To our knowledge, no specific efforts had yet been made to synthesize compounds for *in vivo* application that inhibit AChE by binding solely to PAS.

We described previously a new class of selective mammalian AChE *vs.* butyrylcholinesterase (BChE) inhibitors based on alkylammonium derivatives of 6-methyluracil of acyclic topology, in particular compound (**1**, Fig. 1).[9] Compound **1** and other 1,3-bis[5-(diethyl-*o*-

substitutedbenzyl)pentyl)]-5(6)-substituted uracil derivatives showed a very high affinity for AChE. In the present study, taking compound **1** as a model AChE inhibitor, we attempted to develop AChE inhibitors that specifically bind to the PAS with weak binding to the active site of AChE.

In particular, herein, in continuation of research on new AChE inhibitors among alkylammonium derivatives of 5(6)-substituted uracil derivatives, we synthesized the macrocyclic counterparts of compound **1**, pyrimidinophanes (**2a,b**, **3, 4**, Fig. 1), and investigated them as AChE and BChE inhibitors. Pyrimidinophanes are macrocycles consisting of pyrimidine, and in particular uracil moieties bridged to each other with alkyl spacers.[10] These macrocycles exhibit several biological activities,[10] and it is worth noting their inhibitory action towards enzymes.[11]

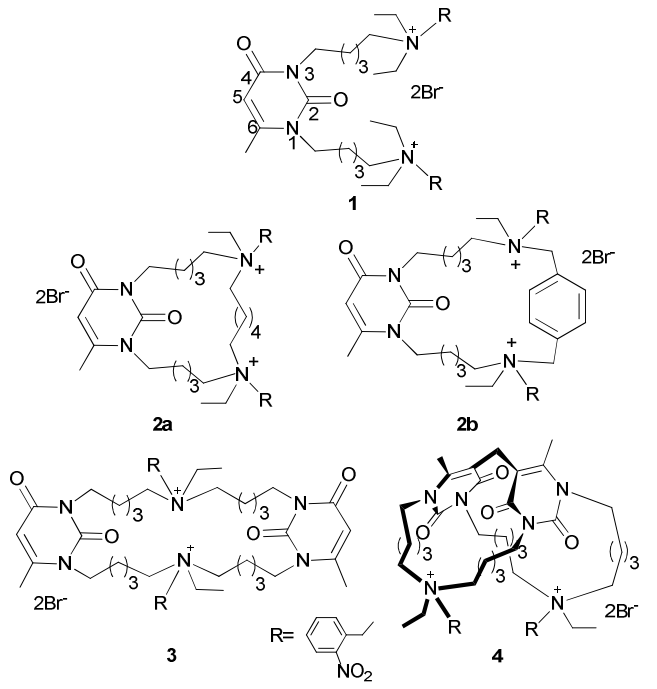

Fig. 1 Structures of acyclic and macrocyclic AChE inhibitors containing the 1,3-bis[5-(o-nitrobenzylethylammonium)pentyl)-6-methyluracilic moiety. In compound **1**, the atom numeration in uracil ring is shown.

Pyrimidinophanes (**2a,b**, **3, 4**) contain the same structural moiety as the acyclic compound **1**, namely 1,3-bis[5-(*o*-nitrobenzylethylammonium)pentyl]-6-methyluracilic unit. These macrocycles can be considered as macrocyclic counterparts of acyclic compounds **1**. It is supposed that restriction in flexibility of the alkylammonium moieties compared to acyclic compound **1** can provide specific binding to AChE, in particular to its PAS. In addition, the alkylammonium moiety can change the type of inhibition of AChE. In our opinion, cyclization of compound **1** make the ligand too bulky to reach the catalytic center of AChE. In order to elucidate structure-activity relationships, the onium groups in pyrimidinophanes were bridged with various spacers. Especially in pyrimidinophanes (**2a**, **2b**), the fragment was cyclized by hexamethylene and *p*-xylylene spacers, respectively, while in pyrimidinophanes (**3**, **4**) 1,3-bis(5-pentyl)-6-methyluracil moiety was used for cyclization of the onium units. Moreover, in macrocycle **4,** an additional methylene bridge was introduced between uracil rings to increase the conformational rigidity of the compound. It is believed that the specific binding of these acyclic and macrocyclic alkylammonium 6-methyluracil derivatives to AChE is tuned by altering (i) topology acyclic or macrocyclic compounds, and (ii) rigidity of the spacers.

Results and discussion

Chemistry

The pyrimidinophanes (**2a,b**, **3, 4**) were synthesized starting from dibromide **5** and diamine **6**, this latter was obtained from **5** and ethylamine. This step was described elsewhere.[12] Cyclization of the diamine **6** with 1,6-dibromohexane and *p*-xylylene dibromide led to pyrimidinophanes (**7a,b**), respectively. Water-soluble pyrimidinophanes (**2a,b**) were prepared by quaternization of the nitrogen atom in bridges of macrocycles **7a,b** with *o*-nitrobenzyl bromide **8** (Scheme1). Pyrimidinophanes (**2a**, **2b**) have 2 chiral centers, and the 4 stereoisomers of each macrocycle can occure. The individual stereoisomers were not isolated, the racemic mixtures of the macrocyclic stereoisomers were used in biological assays.

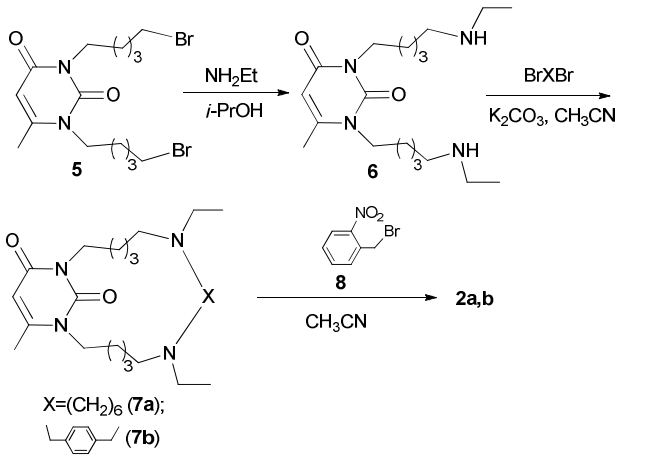

Scheme 1 Synthesis of macrocyclic AChE inhibitors with one 6-methyluracil moiety

Interaction of dibromide **5** with diamine **6** resulted in a mixture of geometric *trans*- and *cis*-isomers, one of them, *cis*-isomer **9,** reacting with *o*-nitrobenzyl bromide **8** gave pyrimidinophane (**3**).[12] Intramolecular methylene bridge between C^5 of the uracil rings of pyrimidinophane (**9**) was introduced by a ring-closure reaction of the macrocycle with paraformaldehyde in aqueous 1.0 M HCl at 140 °C. The product of this reaction, a cryptand-like pyrimidinophane (**10**), was isolated. Recently, we prepared a series of pyrimidinophanes with intra- and intermolecular methylene spacers, using this approach.[13] The last step in Scheme 2 led to the aimed pyrimidinophane **4**.

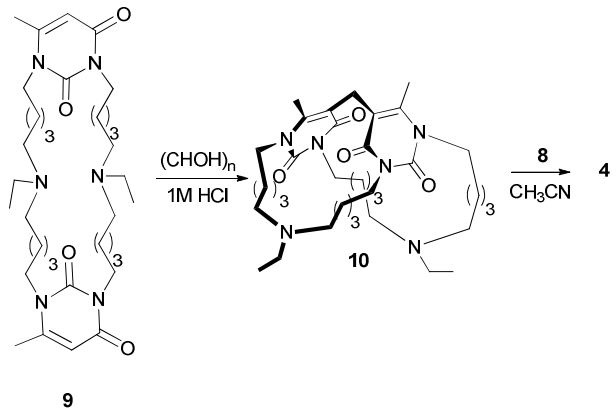

Scheme 2 Synthesis of cryptand-like macrocyclic AChE inhibitor

Pharmacology

The inhibition potency, expressed as IC_{50}, of acyclic and macrocyclic alkylammonium derivatives of 6-methyluracil against AChE and BChE is shown in Table 1.

Table 1 *In vitro* inhibition of AChE from human erythrocytes and human plasma BChE by pyrimidinophanes **2a,b-4** compared to pyridostigmine bromide[a]

Compd	IC_{50} [nM]		AChE selectivity[b]
	AChE	BChE	
1	0.14±0.068	10000±12458.0	66667
2a	59±7.67	9200±1137.4	156
2b	7.0±0.085	1200±175.4	171
3	130±19.5	10000±1124.5	77
4	4000±523.0	20000±2463.6	5
pyridostigminebromide	350±19.6	1000±142.6	3

Values are expressed as mean ± standard error of three independent measurements. Concentration range for the tested compounds was from 10^{-10} to 10^{-5} M (10 concentration points with increments of about a half). [a]Acetylthiocholine and butyrylthiocholine concentration was 2 mM. [b](IC50 BChE)/(IC50 AChE).

Acyclic compound **1** previously synthesized by our group[9] was used as the scaffold for the synthesis of macrocyclic derivatives. It was shown that cyclization of compound **1** into pyrimidinophanes (**2a,b**, **3**, **4**) resulted in decreasing anti-AChE potency. In particular, introduction of the additive uracil moiety (pyrimidinophane (**3**)) and subsequent bridging of both uracil units via a methylene spacer (pyrimidinophane (**4**)) markedly diminished the strength of AChE inhibition compared to compound **1**. Pyrimidinophanes **2a** with hexamethylene spacer showed a decrease in selectivity for AChE *vs* BChE compared to compound **1**. Insertion of the phenyl moiety within the bridge binding nitrogen atoms (pyrimidinophane (**2b**)) slightly improved the inhibitory power towards AChE, thereby increasing the selectivity for AChE *vs* BChE. It should be noted that the affinity of pyrimidinophanes **2a,b** for AChE is in the nanomolar range whereas the difference in inhibition preference for AChE *vs* BChE is of several orders.

The mechanism of AChE inhibition was investigated using acyclic compound **1** and the most active macrocyclic compound, pyrimidinophane (**2b**). Two concentrations of each inhibitor were chosen. For each inhibitor concentration, the initial velocity (V) of substrate hydrolysis was measured at different substrate (S) concentrations ranging from 0.05 to 1 mM. Lineweaver-Burk (L-B) plot, i.e. the reciprocal of initial velocity (1/V) versus the reciprocal of substrate concentration (1/S) was built (Fig. 2, 3). The plot showed that inhibition was non-competitive. Secondary replot of L-B slope versus inhibitor concentration (Fig. 2, insert) provided a good estimate of the inhibition constants, K_I=0.08±0.005 nM for compound **1** and K_I=50.12±1.41 nM for pyrimidinophane **2b**. K_I value for pyrimidinophane **2b** is higher than IC_{50} (Table 1). Cheng and Prusoff described the relationships between IC_{50} and K_i.[14] The fact that K_I>IC_{50} indicates that inhibition is of mixed type with K_{Ic} is higher than K_{Inc}. This situation is described by equation (1) (see Experimental section). Since experiments were performed at [S]>>K_M ([S]=2mM, K_M =0.13mM), equation (1) becomes equation (2) with α= K_{Ic}/K_{Inc}>1. Calculation gave an estimation of α=6.4. This indicates that pyrimidinophane **2b** binds preferentially to ES complex, and inhibits formation of products as a non-competitive inhibitor, i.e. $K_I \approx K_{Inc}$.

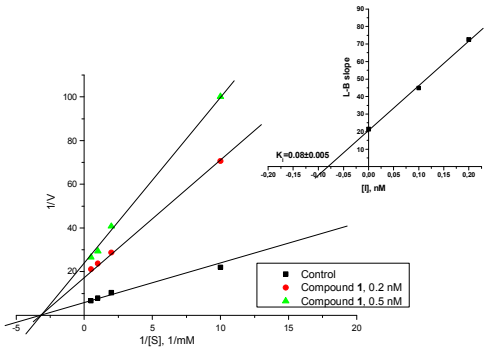

Fig. 2 Reversible inhibition of AChE by compound **1** under steady-state conditions. Double reciprocal plot of initial velocity *vs* substrate concentration in the absence of inhibitor and at two inhibitor concentrations. Insert: secondary replot of L-B plot versus inhibitor concentration.

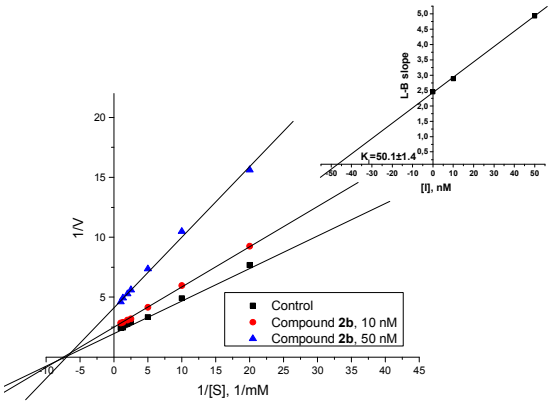

Fig. 3 Reversible inhibition of AChE by pyrimidinophane **2b** under steady-state conditions. Double reciprocal plot of initial velocity *vs* substrate concentration in the absence of inhibitor and at two inhibitor concentrations. Insert: secondary replot of L-B plot versus inhibitor concentration.

Because all studied compounds contain quaternary nitrogen atoms in their structure that impair penetration across the blood-brain barrier, these compounds are of potential interest for treatment of myasthenic syndromes but not for treatment of CNS pathologies.

The potential interest for *in vivo* applications of the most powerful inhibitors compound **1** and pyrimidinophane **2b** was tested for their ability to abolish symptoms of muscle weakness in experimental autoimmune model of myasthenia gravis (EAMG). After EAMG diagnosis, compound **1**, pyrimidinophane **2b**, pyridostigmine bromide or equivalent volume of water were injected intraperitonealy (IP) to rats. The doses of compound **1** and pyrimidinophane **2b** restoring the value of integral muscle action potential (AP) decrement in animals with EAMG to the level of healthy animals was selected. The dose of compound **1** was 0.008 mg/kg, IP (Table 2). This dose is 125 times less than LD_{50} of compound **1** in rats (1 mg/kg, IP). The dose of pyrimidinophane **2b** which restored the level of decrement up to control was 0.3 mg/kg in IP administration (Table 2), what in 50 times lower than LD_{50} of pyrimidinophane **2b** for rats (15.5 mg/kg, IP). Similar effect in EAMG model was achieved by pyridostigmine injection, 0.1 mg/kg (Table 2). This dose is only 27 times lower than LD_{50} of pyridostigmine for rats (2.7 mg/kg, IP). In addition to the toxicity comparable or lower than that of pyridostigmine compound **1** and pyrimidinophane **2b** have another advantage for myasthenia gravis treatment. In addition to its toxicity, lower than that of pyridostigmine, compound **1** and pyrimidinophane **2b** have another advantage for myasthenia gravis treatment. Compound **1** and pyrimidinophane **2b** are more selective for AChE vs. BChE than pyridostigmine (Table 1). The use of specific (AChE) or non-specific (AChE and BChE) inhibitors to treat myasthenia was previously discussed.[15] BChE is abundant in human plasma (average concentration is 50 nM) and present in many cells and organs but its inhibition cannot improve muscle contraction of patients with myasthenia. Clinical studies have indicated that inhibition of plasma BChE may result in potentiating peripheral side effects.[16] Moreover, the activity level of BChE is variable in human populations due to a large genetic polymorphism,[17] and to physiological status. So that doses of BChE inhibitors needed for different patients are different. Thus, non-specific covalent inhibitors, such as pyridostigmine, are more difficult to use because they bind and react first with plasma BChE whose concentration level and reactivity may vary between individuals. The plasma BChE issue does not affect the action of specific AChE inhibitors, especially the action of compound **1** or pyrimidinophane **2b**. Thus, compound **1** and pyrimidinophane **2b** can be considered as a valuable therapeutical candidate for the treatment of pathological muscle weakness syndromes.

Table 2 Decrement of muscle AP amplitude in control group (healthy animals) and in animals with EAMG

Compound, dose, mg/kg	Ratio of 1st to 200th AP amplitudes (decrement), %	
	healthy animals	EAMG animals
Water	95.00±1.00	67.3±2.7
2b, 0.1 mg/kg	-	75.0±1.8
2b, 0.3 mg/kg	-	95.4±1.0
1, 0.004 mg/kg		83.25±1.38
1, 0.008 mg/kg		95.41±0.96
Pyridostigmine bromide, 0.1 mg/kg	-	91.3±1.9

Molecular modeling

In order to explain the different inhibitory properties of compound **1** and its macrocyclic counterparts, pyrimidinophanes, and to clarify their interaction mode in the active center gorge of AChE, molecular docking studies were performed using the X-ray structure 2HA2[18] of murine AChE with succinyldicholine and its half-hydrolyzed product in the active site gorge. This structure solved at 2.05 Å, is the best one among all murine AChE X-ray structures available in the PDB.[19] In addition, the presence of a bifunctional substrate molecule in the gorge makes this structure most suitable for docking of bulky ligands. Due to high number of torsion degrees of freedom in compound **1**, docking parameters were adjusted in series of test runs with succinyldicholine, which displays 11 possible torsions. The selected parameters assured that docked position of succinyldicholine corresponded with X-ray data.

Most favorable binding energies estimated from molecular docking simulations are provided in Table 3. Binding energy can be converted into inhibition constant using standard equation[20] $\Delta G_{bind}=RT\ \ln K_I$, where gas constant R=1.987 cal·K^{-1}·mol^{-1}, and absolute temperature T = 310 K because K_I was determined experimentally at 37°C. For linear compound **1** this gives docking K_I value of 0.212 nM. This calculated value is in a good agreement with experimental value. Indeed, converting experimental K_I value into binding free energy at 310 K we obtain -14.32 kcal/mol. This value differs only by 0.6 kcal/mol from calculated value -13.72 kcal/mol.

Table 3 Binding energy to AChE gorge calculated from molecular docking

Compd	**1**	**2a**	**2b**	**3**	**4**
ΔG_{bind}, kcal/mol	-13.72	-9.45	-10.81	-7.73	-7.36

Compound **1** occupies the whole gorge of AChE from active site to the PAS. In the active site nitro group of one of nitrobenzene ring forms hydrogen bonds both with catalytic serine and oxyanion hole (Gly121 and Gly122), while its phenyl ring is parallel to phenyl ring of Phe338 what ensures

strong π-π interaction between them. Adjacent tetraethylammonium group is surrounded by aromatic rings of Trp86 and Tyr337, establishing strong π-cation interactions with them. There is a hydrogen bond between hydroxyl-group of Tyr124 and oxygen of 6-methyluracyl ring, while the ring itself is parallel to Tyr342 and has strong π-π interaction with it. The second tetraethylammonium group is not far from Trp286, however positioning of its indole ring is not favorable for π-cation interactions. Rather it shows good hydrophobic contact with linker chain between 6-methyluracil ring and the ammonium group. Nitro group of the second nitrophenyl ring establishes hydrogen bonds with side chain and peptide group of Ser293 of the PAS (Fig. 4).

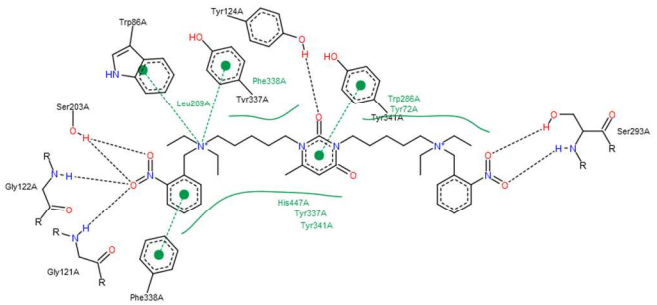

Fig. 4 2D Scheme of position of compound **1** docked inside AChE active site gorge, showing main interactions with amino acid resides. Image generated with PoseView software.

Due to the induced fit step, molecular dynamics simulation of the protein-inhibitor complex final adjustment[21] improved positioning of compound **1** inside the AChE gorge. 30ns MD trajectory revealed the following adjustments in the complex structure (Fig. 5): the tetraethylammonium group located at the bottom of the gorge and the adjacent nitrobenzene ring moved further down the gorge. Then, the tetraethylammonium group formed new strong electrostatic interaction with Glu202, whose carboxylate position moved to fulfill this interaction. As a result, it is interesting to point out that Glu202 formed a hydrogen bond with Tyr133. π-Cation interaction of the tetraethylammonium head with Trp86 was retained, while π-cation interaction with Tyr337 was lost due to displacement of the tetraethylammonium group further down the gorge. Instead, the nitrobenzene ring became in a favorable position to interact with Tyr337. Though the nitrobenzene ring had moved 6Å down the gorge, orientation of the nitro group was still occupying the active center, in immediate proximity of the catalytic Ser203. In the final complex structure, because the 6-methyluracil ring position didn't change at all, it can be concluded that pushing down the tetraethylammonium and nitrobenzene groups resulted from stretching of the linker chain. Tyr124 and Tyr341 moved close to the 6-methyluracil ring for tighter interaction. Important structural change is displacement of Asp74, which in the X-ray structure forms hydrogen bond with Tyr341. After MD simulation, Asp74 is found to be turned away from Tyr341. This allows the second tetraethylammonium group and nitrobenzene ring to move deeper into the PAS and to interact with its components more tightly. Now, compared to the position obtained by docking into the rigid protein, the tetraethylammonium group is facing the indole ring of Trp286, establishing a strong π-cation interaction.

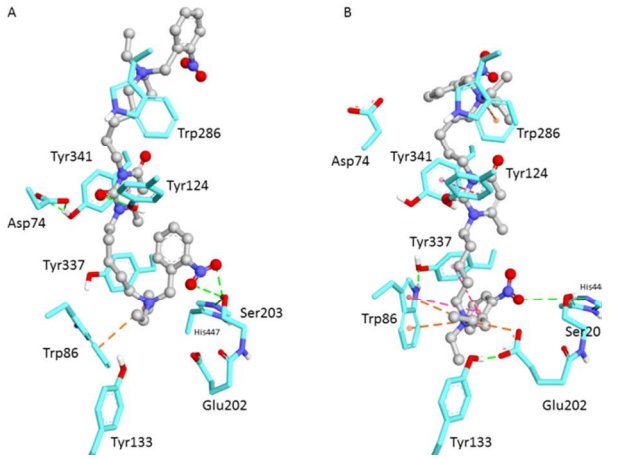

Fig. 5. Position of the compound **1** inside AChE gorge according to (A) molecular docking study with rigid protein and (B) after MD simulation. Carbon atoms of the inhibitor and AChE gorge are shown in grey and cyan, respectively.

Macrocyclic counterparts of compound **1** display considerably lower affinity for AChE. Pyrimidinophanes (**2a**, **2b**) have 2 chiral centers, thus the 4 stereoisomers of each compound were considered. For pyrimidinophanes (**2a,b**) the lowest binding energy among all stereoisomers was provided, in both cases this was (*R,R*)-enantiomer; for **2a** difference in binding energies of all stereoisomers was within 1 kcal/mol, and 1.5 kcal/mol for **2b**. Binding energy calculated for compound **2b** after conversion into inhibition constant gives K_I=23.9 nM. This value is also in good agreement with experimental data. Experimental binding free energy, -10.35 kcal/mol, differs from calculated one by less than 0.5 kcal/mol. Calculated binding energies for other compounds well correlate with measured IC_{50} values.

The most favorable docked position for (*R,R*)-enantiomer of the pyrimidinophane **2b** was deeply inside the gorge, one nitrophenyl ring forming π-π interactions with Trp86 at the bottom of the gorge, and quaternary ammonium group forming π-cation interactions with Phe338 and Tyr337, while the other part of the compound occupied the PAS area (Fig. 6). The other stereoisomers show similar binding energies but were located in PAS and didn't reach the gorge bottom.

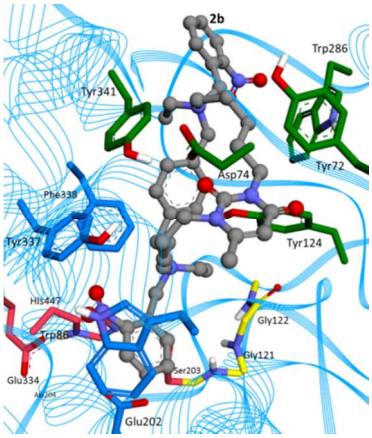

Fig. 6 Molecular docking study on pyrimidinophane **2b** (carbon atoms are grey). Catalytic triad residues (Ser203, His447 and Glu334) are shown in red, catalytic binding sub-site residues (Trp86, Glu202, Tyr337, Phe338) are shown in blue, oxyanion hole residues (Gly121, Gly122 and Ala204) are shown in yellow, peripheral anionic site residues (Tyr72, Asp74, Tyr124, Trp286, Tyr341) are shown in green.

Pyrimidinophane **3** occupies the whole gorge from PAS to active site, in the catalytic anionic sub-site, the nitrophenyl ring is parallel to Trp86 indole ring, that ensures good π-π-interactions; nitro group forms hydrogen bonds with Tyr337 phenolic hydroxyl group; one quaternary ammonium group interacts with Asp74. However, positively charged quaternary ammonium group is located in oxyanion hole, what is rather unfavorable (Fig. 7).

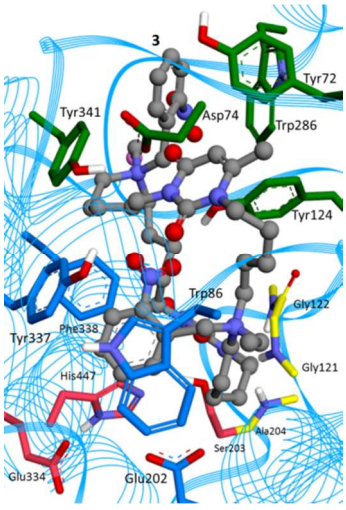

Fig. 7 Molecular docking study on pyrimidinophane **3** (carbon atoms are grey). Catalytic triad residues (Ser203, His447 and Glu334) are shown in red, catalytic binding sub-site residues (Trp86, Glu202, Tyr337, Phe338) are shown in blue, oxyanion hole residues (Gly121, Gly122 and Ala204) are shown in yellow, peripheral anionic site residues (Tyr72, Asp74, Tyr124, Trp286, Tyr341) are shown in green.

For pyrimidinophanes (**2a**, **4**), no position deeply buried in the gorge with good binding energies was found. Instead, in the best docked positions, the macrocycles **2a** ((*R,R*)-enantiomer) and **4** occupy PAS (Fig. 8, 9). Both molecules show the same specific interactions with PAS amino acids: one nitrophenyl ring has π-π interactions with Tyr341, its nitro group forms hydrogen bonds with Phe295 backbone nitrogen, and quaternary ammonium group is located favorably for π-cation interactions with Trp286 ring. However, due to more rigid macrocyclic structure, pyrimidinophane **4** binds to PAS weaker than macrocycle **2a**.

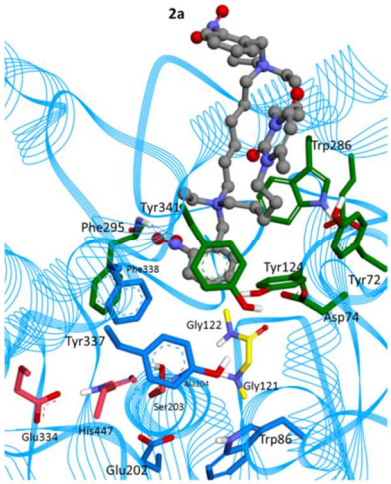

Fig. 8 Molecular docking study on pyrimidinophane **2a** (carbon atoms are grey). Catalytic triad residues (Ser203, His447 and Glu334) are shown in red, catalytic binding sub-site residues (Trp86, Glu202, Tyr337, Phe338) are shown in blue, oxyanion hole residues (Gly121, Gly122 and Ala204) are shown in yellow, peripheral anionic site residues (Tyr72, Asp74, Tyr124, Trp286, Tyr341) are shown in green.

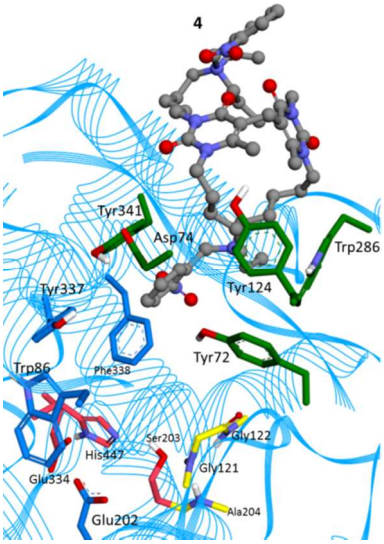

Fig. 9 Molecular docking study on pyrimidinophane **4** (carbon atoms are grey). Catalytic triad residues (Ser203, His447 and Glu334) are shown in red, catalytic binding sub-site residues (Trp86, Glu202, Tyr337, Phe338) are shown in blue, oxyanion hole residues (Gly121, Gly122 and Ala204) are shown in yellow, peripheral anionic site residues (Tyr72, Asp74, Tyr124, Trp286, Tyr341) are shown in green.

Conclusions

In this study we attempted to increase the size of AChE ligands to restrict specific binding to the PAS of AChE. To this aim we synthesized new pyrimidinophanes bearing two *o*-nitrobenzylethyldialkylammonium heads. Almost all of

synthesized pyrimidinophanes inhibited AChE in the nanomolar range. Based on molecular docking simulations, it was suggested that compounds **1, 2b, 3** bind AChE to the active center as well as to the PAS. Compounds **2a**, **4** binds preferentially with PAS. Thus, we found that introduction of the spacer, flexible or rigid, between [5-(*o*-nitrobenzylethylammonium)pentyl] units at N atoms of 6-methyluracil moiety allows to tune the binding of 6-methyluracil derivatives with AChE. In conclusion, it can be stated that pyrimidinophanes **2a** and **4** are promising lead scaffold structures for further design of specific ligands for the PAS of AChE. Also AChE inhibitors with a 6-methyluracil moiety may be considered as potential drugs for the treatment of pathological muscle weakness syndromes.

Acknowledgements

This work was supported by RFBR grant 13-00-40286-K and by the subsidy of the Russian Government to support the Program of Competitive Growth of Kazan Federal University among World's Leading Academic Centers. The authors wish to thank Dr. Al-Shekhadat (Biomedical Center, St. Petersburg, Russia) for synthesis of peptide for induction of EAMG.

Notes and references

[a] A.E. Arbuzov Institute of Organic and Physical Chemistry, Arbuzov str. 8, Kazan 420088, Russia; Fax: (+7)843-273-18-72; E-mail: sve@iopc.ru
[b] N.M. Emanuel Institute of Biochemical Physics, Moscow 119991, Russia
[c] M.V. Lomonosov Moscow State University, Moscow 119991, Russia
[d] Kazan Institute of Biochemistry and Biophysics, Kazan 420111, Russia.
[e] Kazan Federal University, Kazan 420000, Russia
[f] Kazan State Medical University, Kazan 420012, Russia
[g] DYNAMOP, Institut de Biologie Structurale, Grenoble 38000, France

† Electronic Supplementary Information (ESI) available: Synthesis procedures, analytical data and pharmacological methods. See DOI: 10.1039/b000000x/

1 T. Brenner, E. Nizri, M. Irony-Tur-Sinai, Y. Hamra-Amitay and I. Wirguin, *J. Neuroimmunol.*, 2008, **201–202**, 121-127.
2 J. L. Cummings, *Am. J. Psychiatry*, 2000, **157**, 4-15.
3 H. Dvir, I. Silman, M. Harel, T.L. Rosenberry and J.L. Sussman, *Chem. Biol. Interact*., 2010, **187**, 10-22.
4 L. E. Paraoanu and P. G. Layer, *FEBS J*., 2008, **275**, 618-624.
5 M. Singh, M. Kaur, H. Kukreja, R. Chugh, O. Silakari, D. Singh, *Eur. J. Med. Chem*., 2013, **70**, 165-188.
6 S. Olivera-Bravo, I. Ivorra and A. Morales, *British J. Pharmacology*, 2005, **144**, 88-97.
7 E. Karlsson, P. M. Mbugua and D. Rodriguez-Ithurralde, *J. Physiology*, 1984, **79**, 232-240.
8 D. Genest, C. Rochais, C. Lecoutey, J. Sopkova-de Oliveira Santos, C. Ballandonne, S. Butt-Gueulle, R. Legay, M. Since and P. Dallemagne, *Med. Chem. Commun.*, 2013, **4**, 925-931.
9 K. A. Anikienko, E. A. Bychikhin, V. S. Reznik, V. D. Akamsin and I. V. Galyametdinova, *Chem. Biol. Interact*., 2008, **175**, 286-292.
10 V. E. Semenov, *J. Incl. Phenom. Macrocycl. Chem*., 2013, **77**, 1-22.
11 U. Luecking, G. Siemeister, M. Schaefer, H. Briem, M. Krueger, P. Lienau and P. Jautela, *ChemMedChem*, 2007, **2**, 63-77.
12 V. E. Semenov, A. D. Voloshina, E. M. Toroptzova, N. V. Kulik, V. V. Zobov, R. Kh. Giniyatullin, A. S. Mikhailov, A. E. Nikolaev, V. D. Akamsin and V. S. Reznik, *Eur. J. Med. Chem*., 2006, **41**, 1093-1101.
13 V. E.Semenov, R. Kh. Giniyatullin, A. S. Mikhailov, A. E. Nikolaev, S. V. Kharlamov, S. K. Latypov and V. S. Reznik, *Eur. J. Org. Chem*., 2011, **28**, 5423-5426.
14 Y. Cheng and W. H. Prusoff, *Biochem. Pharmacology*, 1973, **22**, 3099-3108.
15 M. Komloova, K. Musilek, M. Dolezal, F. Gunn-Moore and K. Kuca, *Curr. Med. Chem.*, 2010, **17**, 1810‑1824.
16 E. C. Hulme, N. J. M. Birdsall and N. J. Buckley, *Ann. Rev. Pharmacol. Toxicol*., 1990, **30**, 633-673.
17 B. Benyamin, R. P. Middelberg, P. A. Lind, A. M. Valle, S. Gordon, D. R. Nyholt, S. E. Medland, A. K. Henders, A. C. Heath, P. A. F. Madden, P. M. Visscher, D. T. O'Connor, G. W. Montgomery, N. G. Martin and J. B. Whitfield, *Hum. Mol. Genet*., 2011, **20**, 4504‑4514.
18 Y. Bourne, Z. Radic, G. Sulzenbacher, E. Kim, P. Taylor and P. Marchot, *J. Biol. Chem*., 2006, **281**, 29256-29267.
19 H.M. Berman, J. Westbrook, Z. Feng, G. Gilliland, T. N. Bhat, H. Weissig, I. N. Shindyalov and P. E. Bourne, *Nucl. Acids Res*., 2000, **28**, 235-242.
20 G. M. Morris, D. S. Goodsell, R. S. Halliday, R. Huey, W. E. Hart, R. K. Belew and A. J. Olson, *J. Am. Chem. Soc*., 1998, **19**, 1639-1662.
21 This work "Slow, tight-binding inhibition of acetylcholinesterase by alkylammonium derivatives of 6-methyluracil: a molecular dynamics study" is currently under preparation, and it will be detailed elsewhere.